

Electron-Phonon Interactions in C_{28} -derived Molecular Solids

Nichols A. Romero,¹ Jeongnim Kim,² and Richard M. Martin¹

¹*Department of Physics, Materials Research Laboratory,
and Materials Computation Center, University of Illinois, Urbana, IL 61801*

²*NCSA, Materials Research Laboratory, and Materials Computation Center, University of Illinois, Urbana, IL 61801*

(Dated: August 27, 2004)

We present *ab initio* density-functional calculations of molecular solids formed from C_{28} -derived closed-shell fullerenes. Solid $C_{28}H_4$ is found to bind weakly and exhibits many of the electronic structure features of solid C_{60} with an enhanced electron-phonon interaction potential. We show that chemical doping of this structure is feasible, albeit more restrictive than its C_{60} counterpart, with an estimated superconducting transition temperature exceeding those of the alkali-doped C_{60} solids.

PACS numbers: 74.10.+v, 71.15.Mb, 74.25.Jb, 74.70.Wz

There continues to be intense research efforts in studying fullerenes for their diverse properties, not the least of which is their unusually high superconducting transition temperatures T_c (up to 40 K in Cs_3C_{60}).¹ Theoretical studies show that many of the phenomena associated with this class of materials can be explained within the electron-phonon mediated picture of superconductivity.^{2,3,4,5,6} The high T_c of these materials relative to that of intercalated graphite is attributed to the curvature of C_{60} .^{3,7,8} Hence, solids based on smaller fullerenes possessing an electronic structure similar to that of alkali-doped C_{60} may exhibit a T_c enhancement.

The goal of the present work is to identify new molecular solids analogous to the alkali-doped C_{60} solids with similar electronic structure and increased electron-phonon coupling. We consider solids composed of C_{28} -derived closed-shell molecules ($C_{24}B_4$, $C_{24}N_4$, and $C_{28}H_4$) which can potentially have a large tunable density-of-states (DOS) arising from the narrow weakly broadened bands. Theoretical studies of the isolated molecules indicate that they should be stable,^{9,10,11,12} however, to our knowledge there are no studies of their solid forms. Here we present results of *ab initio* pseudopotential density-functional calculations to determine the structural and electronic properties of the solids in pristine and doped forms. There have been *ab initio* studies of solids based on C_{28} (Refs. 13,14,15) and C_{36} ,^{16,17} which exhibit increased electron-phonon coupling. However, these molecules form covalent solids differently from C_{60} . We find that $C_{24}B_4$ and $C_{24}N_4$ also form strongly-bonded solids, but that $C_{28}H_4$ exhibits many of the salient features of solid C_{60} . Several doping scenarios are investigated for alkali doped $C_{28}H_4$ crystals, and a promising candidate is identified for high T_c .

First proposed by Kroto,¹⁸ the C_{28} molecule obeys the T_d point group. This fullerene is produced with an abundance nearly as great as that of C_{60} in the laser vaporization of graphite.¹⁹ It is a very reactive molecule with dangling bonds localized on each of the four apex atoms shown in black for each C_{28} in Fig. 1(a). Because the C_{28} molecule is a tetravalent superatom, a reasonable candidate for a solid is a four-fold coordinated diamond-

like structure. The C_{28} molecules can be four-fold coordinated with respect to the tetrahedron apexes as in Fig. 1(a) *apex-bonded* or with respect to the tetrahedron faces as in Fig. 1(b) *face-bonded*. Since the C_{28} molecules have dangling bonds localized on the tetrahedron apexes, the lower energy structure will be the former. Previous *ab initio* calculations^{14,15} have shown that the covalent bonds of the apex-bonded C_{28} hyperdiamond are very strong compared to the weak forces responsible for bonding in solid C_{60} .

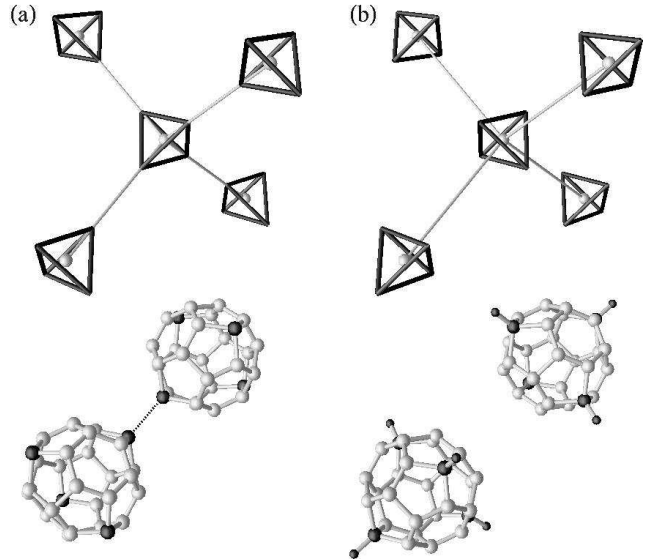


FIG. 1: Schematic diagrams of the first nearest neighbors in the hyperdiamond structures (top) with examples of pairs of C_{28} -derived molecules shown below. The lattice sites in the solid are highlighted by the grey spheres enclosed in the tetrahedra. The two distinct orientations of the constituent molecules are represented by those of the tetrahedra. The nearest-neighbor pairs show two distinct bonding configurations: (a) *apex-bonded* C_{28} hyperdiamond forms covalent bonds (dotted line) between apex atoms colored in black; (b) *face-bonded* $C_{28}H_4$ hyperdiamond forms weak bonds between six-membered rings with hydrogen atoms depicted as smaller black spheres.

In search of suitable molecular solids, we study hyperdiamond structures constructed from three distinct closed-shell molecules – $C_{24}B_4$, $C_{24}N_4$, and $C_{28}H_4$, using *ab initio* pseudopotential density functional methods within the local density approximation (LDA). The SIESTA code^{20,21} was used to perform conjugate gradient minimization of forces and stresses to find relaxed structures. Though other possible solid structures for C_{28} have been proposed,²² they are reported to be higher in energy than apex-bonded hyperdiamond and so were not considered in this study. Although all three molecules are stable, as was found previously,^{9,10,11,12} we find that in the solid the $C_{24}B_4$ molecules are unstable and break apart. Of the two geometries investigated for $C_{24}N_4$, apex-bonded hyperdiamond is much lower in energy forming a covalent solid like C_{28} . The face-bonded $C_{24}N_4$ hyperdiamond is higher in energy and in addition shows significant hybridization in the conduction band. Thus neither $C_{24}B_4$ nor $C_{24}N_4$ were suitable candidates for reproducing the electronic structure of solid C_{60} .

The $C_{28}H_4$ molecule is found to be stable in the solid. Because the dangling bonds are passivated by hydrogen, apex-bonded $C_{28}H_4$ hyperdiamond (and other suggested structures²²) are not favorable; the lower energy structure is the face-bonded $C_{28}H_4$ hyperdiamond shown in Fig. 1(b). The latter is predicted to be a weakly bound solid with a lattice constant of 16.3 Å and a binding energy of approximately 0.2 eV per $C_{28}H_4$ molecule. The bonding between the six-membered rings is similar to that found for some orientations of C_{60} molecules.²³ The structural and electronic properties of face-bonded $C_{28}H_4$ hyperdiamond in both its pristine and doped forms are the subject for the remainder of this paper.

Figure 2 compares the band structure and DOS between solid C_{60} and $C_{28}H_4$ around the band gap. The valence (conduction) band is formed from the three-fold degenerate LUMO (HOMO) of the $C_{28}H_4$ molecule. The weakly broadened bands bear a striking similarity to those found in solid C_{60} . Undoped solid $C_{28}H_4$ forms an insulator with 1-eV direct gap at Γ . Upon chemical doping, the Fermi energy is expected to fall within a DOS peak with a value comparable to the alkali-doped C_{60} materials.

The dimensionless electron-phonon coupling parameter $\lambda = N(0)V_{ep}$ depends on both the DOS at the Fermi energy $N(0)$ and the electron-phonon interaction potential V_{ep} which is proportional to the curvature of the fullerene.^{3,7,8} That $C_{28}H_4$ is more curved than C_{60} suggests that higher transition temperatures are obtainable. In general, V_{ep} can be calculated as a double sum over the Fermi surface connecting states due to the phonon deformation potential. For molecular solids like C_{60} and $C_{28}H_4$, the small dispersion of the electronic and phononic spectra implies that the molecular states and intramolecular phonons are an excellent approximation to those found in the solid.^{2,3,5} Therefore, we compute V_{ep} for solid $C_{28}H_4$ by only considering the intramolecular phonon coupling to the molecular states.

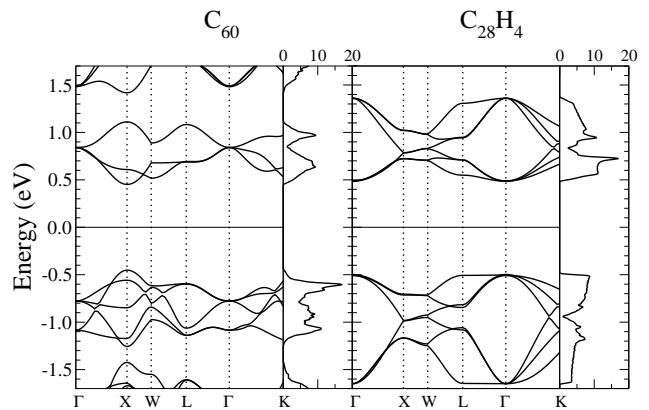


FIG. 2: Comparison of the band structure and DOS (states/eV/spin/cell) between solid fcc-Fm $\bar{3}$ C_{60} and face-bonded $C_{28}H_4$ hyperdiamond. For $C_{28}H_4$ solid, the set of six bands above and below the gap are derived respectively from the three-fold degenerate LUMO and HOMO for each $C_{28}H_4$ in the two-molecule cell. The thin solid lines at zero show the centers of the direct gaps.

The electron-phonon interaction potential is evaluated for the three-fold degenerate LUMO using the phonon frequencies ω_ν and eigenvectors ε_ν for the isolated $C_{28}H_4$ molecule. Since our fullerene is composed of multiple species, it is convenient to include the mass of each species into the phonon eigenvectors normalization, $\sum_i^{\mathcal{N}} \varepsilon_\nu^{i\dagger} \cdot \varepsilon_\nu^i M_i = \delta_{\nu\nu'}$, where \mathcal{N} is the number of atoms in the fullerene. The electron-phonon interaction potential can be extracted from λ ²⁴ and written in the form

$$V_{ep} = \frac{1}{g^2} \sum_\nu \frac{1}{\omega_\nu^2} \sum_{\alpha, \alpha'}^g |\langle \alpha | \sum_i^{\mathcal{N}} \varepsilon_\nu^i \cdot \nabla_i V | \alpha' \rangle|^2, \quad (1)$$

where α and α' are the molecular states with degeneracy g for which the coupling is being evaluated. The matrix element in Eq. (1) is evaluated by a finite-difference approach where the deformation potential is calculated within the frozen-phonon scheme. Our calculated value of V_{ep} is 181 meV, which includes contributions from most of the intramolecular phonons. It is observed in Raman-scattering experiments^{25,26} and predicted by theory^{5,27} that the A_g phonons are screened out in alkali-doped C_{60} . In the case of $C_{28}H_4$, the A_g phonons contribute 12 meV to V_{ep} . Even taking into account the screening of the A_g phonons, the electron-phonon interaction potential for $C_{28}H_4$ is over twice as large as that of C_{60} (63 meV).¹⁶

In Fig. 2 we see that analogous to C_{60} , solid $C_{28}H_4$ is an insulator and can not superconduct unless doped. *Ab initio* calculations of alkali-doped C_{60} have demonstrated that intercalation of alkali atoms into the tetrahedral and octahedral sites result in the donation of the alkali valence electrons to the C_{60} conduction band.^{3,28,29,30} This is reflected in the band structure by a lack of hybridiza-

tion of the alkali states with the conduction band, so that the band structure of the superconducting alkali-doped C_{60} differs from that of pristine C_{60} primarily by a rigid shift in the Fermi energy. This is viewed as the ideal doping case which we seek in the smaller fullerene solids.

We have studied doping of solid $C_{28}H_4$ with the alkali Na; other alkali atoms are expected to behave similarly. The intercalation of Na atoms into the solid $C_{28}H_4$ was investigated in three different scenarios: (a) $NaC_{28}H_4$ intercalation into the tetrahedral site; (b) $Na_2C_{28}H_4$ intercalation into the interstitial site between the six-membered rings on nearest neighbor $C_{28}H_4$ molecules; (c) $Na@C_{28}H_4$ endohedral doping. In each case, the Na-doped $C_{28}H_4$ structures were relaxed by conjugate gradient minimization of forces and stresses. We discuss the effects of doping as they pertain to the crystal structure, electronic properties and enthalpies of reaction.³⁶

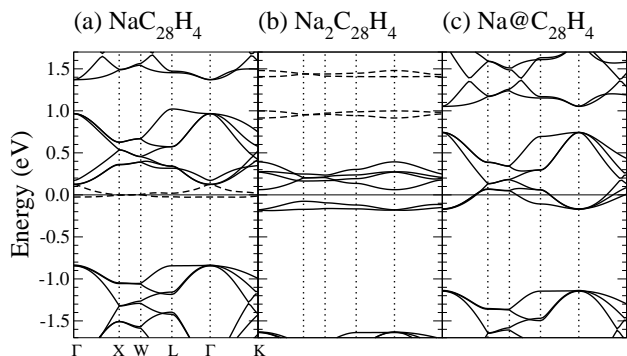


FIG. 3: Band structure comparison among three doping cases (a) Intercalation of Na atoms into tetrahedral site; (b) Intercalation of Na atoms into the interstitial sites between opposing six-membered rings on nearest neighbor $C_{28}H_4$; (c) Encapsulation of Na atom into the $C_{28}H_4$ cage. Dopant bands are depicted by dashed lines. The thin solid line at zero is the Fermi level.

The intercalation of Na atoms into the tetrahedral site occurs with no significant expansion of the lattice [similar to that found, e.g., in K_3C_{60} (Ref. 31)]. However, unlike the C_{60} fullerenes, additional bands appear just below the conduction band of $C_{28}H_4$ as depicted by the dashed lines in Fig. 3(a). A Mulliken population analysis reveals that the H atoms of the $C_{28}H_4$ gain additional charge, which is reasonable since four H atoms point into each tetrahedral site of solid $C_{28}H_4$ where a Na atom is located. Hence, in the $NaC_{28}H_4$ there is no doping of the conduction band; instead the H and Na states hybridize to form dopant states at the Fermi level. Furthermore, the calculated enthalpy of reaction indicates that the compound is not stable, so that this doping scenario would not be expected to occur naturally.

Intercalation of Na atoms into the interstitial site between opposing six-membered rings on nearest neighbor

molecules results in a doping ratio twice as high as that of the previous case. Unlike $NaC_{28}H_4$, there no longer are any dopant bands near the Fermi level. We determine the enthalpy of reaction to be -0.9 eV per Na atom which is in line with those calculated for K_3C_{60} .³¹ When the cell stress is relaxed, the lattice constant of $Na_2C_{28}H_4$ increases from 16.3 Å to 18.1 Å resulting in a narrowing of the bands. In Fig. 3(b), we see the opening of a 0.2 -eV gap at the Fermi level and so the solid transforms from a conductor into an insulator with a small gap upon cell relaxation. This is a direct result of Jahn-Teller distortion of the doped $C_{28}H_4$ molecules whose symmetry is reduced from T_d to D_{2d} . The Jahn-Teller distortion of the isolated charged $C_{28}H_4$ molecule splits the 3-fold degenerate LUMO into a twofold degenerate and onefold degenerate state with a 0.2 -eV gap. Hence, when the forces-and-stresses are relaxed in $Na_2C_{28}H_4$, a band gap similar in size to the Jahn-Teller gap opens up at the Fermi level. Thus in this case, doping by intercalation leads to insulating behavior.

The encapsulation of Na atom into the $C_{28}H_4$ cage is the doping scenario which most closely parallels that of the alkali-doped C_{60} solids. Figure 3(c) depicts a simple rigid shift of the Fermi level into the conduction band of $C_{28}H_4$. In contrast to $Na_2C_{28}H_4$, the lattice constant of $Na@C_{28}H_4$ does not increase. The Na atom is located at the center of the $C_{28}H_4$ and we find no Jahn-Teller distortion. Although the isolated charged $C_{28}H_4$ molecule undergoes a Jahn-Teller distortion due to the degeneracy of the LUMO state, the broadening of the bands in $Na@C_{28}H_4$ is found to be sufficient to eliminate this effect. Since it is known that endohedrally-doped C_{28} can be formed,¹⁹ the relevant enthalpy of reaction for this system is the total energy of solid $Na@C_{28}H_4$ relative to the isolated molecules; we find that this solid can be formed with an enthalpy of reaction similar to that of undoped $C_{28}H_4$.³⁷

Within the electron-phonon mediated theory of superconductivity, $\lambda = N(0)V_{ep}$ plays a crucial role in determining T_c . The superconducting transition temperature for $Na@C_{28}H_4$ can be estimated using McMillan's solution of the Eliashberg equations,^{32,33}

$$T_c = \frac{\omega_{ln}}{1.2} \exp \left[-\frac{1.04(1 + \lambda)}{\lambda - \mu^*(1 + 0.62\lambda)} \right] \quad (2)$$

where ω_{ln} is a typical phonon frequency and μ^* is the Coulomb pseudopotential which describes the effective electron-electron repulsion. Typical values of $\omega_{ln} \approx 10^3$ K for $C_{28}H_4$ and C_{60} . We may expect that μ^* for $C_{28}H_4$ should not differ considerably from that of C_{60} since the subbands and phonon energies are similar. For alkali-doped C_{60} solids, experimental results lead to $\mu^* \approx 0.22$.³⁴ The endohedral doping scenario for $C_{28}H_4$ gives that $N(0) \approx 5$ states/eV/spin/molecule which is half of that found in the canonical alkali-doped C_{60} structure, i.e., K_3C_{60} .³¹ Accounting for screening of the A_g phonons in the electron-phonon interaction, a $V_{ep} = 169$ meV gives an enhancement factor of

$\lambda(\text{Na}@C_{28}H_4) \approx 1.5\lambda(\text{K}_3C_{60})$.³⁸ These approximations are in line with those found in the literature^{6,13,16} and is sufficient for qualitative comparison. Using this value of μ^* and ω_{in} , one finds that $\lambda(\text{K}_3C_{60}) = 0.84$ in order to explain the experimentally observed $T_c(\text{K}_3C_{60}) = 19.3$ K.³⁵ The enhancement factor for λ that we calculate predicts a $T_c(\text{Na}@C_{28}H_4) \approx 3T_c(\text{K}_3C_{60}) \approx 58$ K, higher than that found in the highest temperature alkali-doped fulleride [40 K in Cs_3C_{60} (Ref. 1)].

In summary, *ab initio* pseudopotential density functional calculation were performed on C_{28} -derived molecular solids. We find a $C_{28}H_4$ solid which binds weakly and exhibits many of the band structure features as C_{60} . Several doping scenarios are investigated and we find that $\text{Na}@C_{28}H_4$ to be the most promising for superconductivity. The calculated electron-phonon interaction potential and DOS leads to a T_c enhancement of three times that

found in K_3C_{60} . Since endohedral doping is expected to be insensitive to the type of dopant, this suggests promising possibilities with other atoms including ones of higher valence that can control the doping level. Guo *et al.*¹⁹ have succeeded in encapsulating group-IVB atoms in C_{28} , which suggests that other small fullerenes such as $C_{28}H_4$ can also be endohedrally doped.

We are grateful to J. Gale, P. Ordejón, E. Koch, L. Mitás, M. Côté, and J. L. Martins for useful discussions. We are also very thankful to K. Delaney for providing critical readings of this manuscript. This work was supported by National Science Foundation Grant No. DMR-9976550 and by the U.S. Department of Energy under Contract No. DEFG-96-ER45439. This work utilized the NCSA IBM pSeries 690, the PSC HP Alphaserver cluster and the MCC IBM RS/6000 cluster.

-
- ¹ T. T. M. Palstra, O. Zhou, Y. Iwasa, P. E. Sulewski, R. M. Fleming, and B. R. Zegarski, *Solid State Commun.* **93**, 327 (1995).
 - ² C. M. Varma, J. Zaanen, and K. Raghavachari, *Science* **254**, 989 (1991).
 - ³ M. Schluter, M. Lannoo, M. Needels, G. A. Baraff, and D. Tománek, *Phys. Rev. Lett.* **68**, 526 (1992).
 - ⁴ I. I. Mazin, S. N. Rashkeev, V. P. Antropov, O. Jepsen, A. I. Liechtenstein, and O. K. Andersen, *Phys. Rev. B* **45**, 5114 (1992).
 - ⁵ V. P. Antropov, O. Gunnarsson, and A. I. Liechtenstein, *Phys. Rev. B* **48**, 7651 (1993).
 - ⁶ O. Gunnarsson, *Rev. Mod. Phys.* **69**, 575 (1997).
 - ⁷ V. H. Crespi, *Phys. Rev. B* **60**, 100 (1999).
 - ⁸ J. L. Martins, *Europhys. News* **23**, 32 (1992).
 - ⁹ T. Guo, R. E. Smalley, and G. E. Scuseria, *J. Chem. Phys.* **99**, 352 (1993).
 - ¹⁰ E. Kaxiras, K. Jackson, and M. R. Pederson, *Chem. Phys. Lett.* **225**, 448 (1994).
 - ¹¹ Y. N. Makurin, A. A. Sofronov, A. I. Gusev, and A. L. Ivanovsky, *Chem. Phys.* **270**, 292 (2001).
 - ¹² D. F. T. Tuan and R. M. Pitzer, *J. Phys. Chem.* **100**, 6277 (1996).
 - ¹³ N. Breda, R. A. Broglia, G. Coló, G. Onida, D. Provasi, and E. Vigezzi, *Phys. Rev. B* **62**, 130 (2000).
 - ¹⁴ D. M. Bylander and L. Kleinman, *Phys. Rev. B* **47**, 10967 (1993).
 - ¹⁵ E. Kaxiras, L. M. Zeger, A. Antonelli, and Y. M. Juan, *Phys. Rev. B* **49**, 8446 (1994).
 - ¹⁶ M. Côté, J. C. Grossman, M. L. Cohen, and S. G. Louie, *Phys. Rev. Lett.* **81**, 697 (1998).
 - ¹⁷ J. C. Grossman, S. G. Louie, and M. L. Cohen, *Phys. Rev. B* **60**, R6941 (1999).
 - ¹⁸ H. Kroto, *Nature* **329**, 529 (1987).
 - ¹⁹ T. Guo, M. D. Diener, Y. Chai, M. J. Alford, R. E. Haufler, S. M. McClure, T. Ohno, J. H. Weaver, G. E. Scuseria, and R. E. Smalley, *Science* **257**, 1661 (1992).
 - ²⁰ J. M. Soler, E. Artacho, J. D. Gale, A. Garcia, J. Junquera, P. Ordejón, and D. Sánchez-Portal, *J. Phys.: Condens. Matter* **14**, 2745 (2002).
 - ²¹ P. Ordejón, E. Artacho, and J. M. Soler, *Phys. Rev. B* **53**, 10441 (1996).
 - ²² J. Kim, G. Galli, J. W. Wilkins, and A. Canning, *J. Chem. Phys.* **108**, 2631 (1998).
 - ²³ O. Gunnarsson, S. Satpathy, O. Jepsen, and O. K. Andersen, *Phys. Rev. Lett.* **67**, 3002 (1991).
 - ²⁴ D. Rainer, *Prog. Low Temp. Phys.* **10**, 371 (1986).
 - ²⁵ S. J. Duclos, R. C. Haddon, S. Glarun, A. F. Hebbard, and K. B. Lyons, *Science* **254**, 1625 (1991).
 - ²⁶ T. Pichler, M. Matus, J. Kürti, and H. Kuzmany, *Phys. Rev. B* **45**, 13841 (1992).
 - ²⁷ M. Schluter, M. Lannoo, M. Needels, G. A. Baraff, and D. Tománek, *J. Phys. Chem. Solids* **53**, 1473 (1992).
 - ²⁸ J. L. Martins and N. Troullier, *Phys. Rev. B* **46**, 1766 (1992).
 - ²⁹ W. Andreoni, P. Giannozzi, and M. Parrinello, *Phys. Rev. B* **51**, 2087 (1995).
 - ³⁰ S. Satpathy, V. P. Antropov, O. K. Andersen, O. Jepsen, O. Gunnarsson, and A. I. Liechtenstein, *Phys. Rev. B* **46**, 1773 (1992).
 - ³¹ J. L. Martins and N. Troullier, *Phys. Rev. B* **46**, 1766 (1992).
 - ³² W. C. McMillan, *Phys. Rev.* **167**, 331 (1968).
 - ³³ G. M. Eliashberg, *Zh. Éksp. Teor. Fiz.* **38**, 966 (1960).
 - ³⁴ M. S. Fuhrer, K. Cherrey, A. Zettl, M. L. Cohen, and V. H. Crespi, *Phys. Rev. Lett.* **83**, 404 (1999).
 - ³⁵ K. Holczer, O. Klein, S. M. Huang, R. B. Kaner, K. J. Fu, R. L. Whetten, and F. Dieferich, *Science* **252**, 1152 (1991).
 - ³⁶ The enthalpy of reaction is referenced to the relevant constituents, the calculated total energy of solid $C_{28}H_4$ and bcc sodium metal, unless otherwise noted. Negative values for the enthalpy indicate that the compounds are stable with respect to the reference system.
 - ³⁷ When isolated molecules are the reference system, the enthalpy of reaction differs from the binding energy by only a minus sign.
 - ³⁸ The enhancement factor was determined using $V_{\text{ep}} = 63$ meV for C_{60} from Côté *et al.* (Ref. 16) and using the calculated values of $N(0)$ for K_3C_{60} and $\text{Na}@C_{28}H_4$, which are in the ratio of 2:1, as discussed in the text.